

CrystEngComm

Accepted Manuscript



This is an *Accepted Manuscript*, which has been through the Royal Society of Chemistry peer review process and has been accepted for publication.

Accepted Manuscripts are published online shortly after acceptance, before technical editing, formatting and proof reading. Using this free service, authors can make their results available to the community, in citable form, before we publish the edited article. We will replace this *Accepted Manuscript* with the edited and formatted *Advance Article* as soon as it is available.

You can find more information about *Accepted Manuscripts* in the [Information for Authors](#).

Please note that technical editing may introduce minor changes to the text and/or graphics, which may alter content. The journal's standard [Terms & Conditions](#) and the [Ethical guidelines](#) still apply. In no event shall the Royal Society of Chemistry be held responsible for any errors or omissions in this *Accepted Manuscript* or any consequences arising from the use of any information it contains.



ARTICLE

Understanding the Roles of Metal Sources and Dodecanethiols in the Formation of Metal Sulfide Nanocrystals via a Two-Phase Approach

Received 00th January 20xx,
Accepted 00th January 20xx

DOI: 10.1039/x0xx00000x

www.rsc.org/

Miao Wang,^a Aiwei Tang,^{† a b} Dongxu Zhu,^a Chunhe Yang,^a Feng Teng^b

We present a two-phase approach for controllable synthesis of metal sulfide nanocrystals, such as Cu_{2-x}S , Ag_2S and Ni_3S_2 , in which the reaction takes place at the water/oil interface. This method is environmental-friendly and economical due to the use of low-toxic and low-cost reagents. The crystal phase and composition can be manipulated by varying the amount of *n*-dodecanethiols (DDT) in organic phase and the type of metal salts in aqueous phase. For example, the CuO nanocrystals can be obtained in the presence of low DDT concentration and the hydroxyl ions, and Cu_{2-x}S nanocrystals are successfully synthesized in the presence of relatively high DDT concentration. The XPS spectra and near-infrared (NIR) absorption spectra have been employed to confirm the formation of CuO and Cu_{2-x}S nanocrystals. Moreover, the Cu_{2-x}S nanocrystals often exhibit an obvious localized surface plasmon resonance band due to their excess free holes in the valence band. A plausible formation mechanism has been proposed to study the synthesis of Cu_{2-x}S and CuO nanocrystals. This two-phase approach has also been extended to prepare Ag_2S and Ni_3S_2 nanocrystals, and the Ag and Ag_2S nanocrystals often coexist in the products which are in close associated with the cleavage of S–C bonds or Ag–S bond, which relies on the DDT dosage and the reactivity of metal sources. This two-phase approach may open up a simple and environmental-friendly strategy for synthesis of metal sulfide nanocrystals with controllable crystal phase and morphology.

1. Introduction

Colloidal inorganic nanocrystals have attracted much attention due to their unique optical, electrical properties and their wide potential applications in the different fields of optoelectronics and biomedicines during the past few decades.^{1–8} As an important category of colloidal semiconductor nanocrystals, metal sulfide nanocrystals have been extensively studied due to their amazing size- and shape-dependent chemical and physical properties, which have become promising candidates in the light-emitting diodes, solar cells, memory devices and biological labels.^{9–17} In recent years, nanostructured copper- and silver-based sulfides have been regarded as lucrative alternatives to the existing metal sulfide nanocrystals containing highly toxic elements since their intrinsic environmental-friendly advantages and the non-negligible optoelectronic properties.^{18–24} To date, different colloidal synthetic methods have been developed to prepare copper sulfide (Cu_{2-x}S) and silver sulfide (Ag_2S) nanocrystals, in which their morphology,

crystal phase and composition could be precisely controlled by manipulation of the reaction conditions.^{25–32}

Among various kinds of colloidal chemical approaches for synthesis of metal sulfide nanocrystals, a two-phase strategy is a powerful approach for fabrication of different low-dimensional nanocrystals because of its low cost and environmental benignity, in which the nucleation and growth of the nanocrystals occurs at the water-oil interface.^{33, 34} As compared to one-phase colloidal chemical approaches, such as the hot-injection and single-source precursor decomposition methods, a relatively slow nucleation and growth takes place in the two-phase strategy, which is favorable for the formation of uniform nanostructures.^{33, 35} Pan et al successfully synthesized highly luminescent and nearly monodisperse CdS nanocrystals via a two-phase approach, in which cadmium-myristic acid and *n*-trioctylphosphine oxide (TOPO) in toluene were used as the cadmium source, and the low reactive thiourea in water was acted as the sulfur source. The CdS nanocrystals synthesized by the two-phase experienced a longer nucleation and growth period as compared with that made by the hot-injection approach.^{35–38} Moreover, Li's group developed a novel water-oil interface confined route to prepare Cu_2S nanocrystals and study the self-assembly behavior. In the reaction, the aqueous solution of copper salts and other anions were used as copper sources and DDT was used as the organic phase which acted as the sulfur source, surface ligands and the reducer.³⁹ This work focused on the self-assembly of Cu_2S nanocrystals on the water-oil interface, however, the formation mechanism of the Cu_2S nanocrystals is still unclear, such as the effects of the dosage of DDT and the different reactivity of copper sources on the nucleation and growth of the Cu_2S nanocrystals. Therefore, it is still interesting to study the formation mechanism of metal sulfide nanocrystals synthesized by a two-phase approach.³⁹

^a Department of Chemistry, school of science, Beijing JiaoTong University, Beijing 100044, PR China. E-mail: awtang@bjtu.edu.cn; Tel: +86-10-51683627

^b Key Laboratory of Luminescence and Optical Information, Ministry of Education, Beijing JiaoTong University, Beijing 100044, PR China.

[†] Electronic supplementary information (ESI) available: The size distribution histograms of the products synthesized by using different Cu sources in the presence of different dosage of DDT, the FTIR and EDS spectra of the products synthesized using 5 mL of DDT, the TEM images and XRD patterns of the products synthesized in the presence of other added anions or using different copper salts, the absorption spectra of the products synthesized with or without toluene in the organic phase as well as the XRD and TEM images of the products synthesized using $\text{Ag}(\text{NH}_3)^+$ as Ag sources. See DOI: 10.1039/x0xx00000x

In this work, a simple two-phase approach has been developed to synthesize Cu_{2-x}S , Ag_2S and Ni_9S_8 nanocrystals, in which pure DDT or DDT in toluene is selected as organic phase, and the different types of metal salts in water are used as aqueous phase, thus the two kinds of precursors are separated spatially in the two phases. The effects of the DDT concentrations on the formation of Cu_{2-x}S nanocrystals have been studied in detail, and the DDT was found to act as surface ligands, sulfur source and reducing agent. The reactivity of the metal salts, such as cuprammouium compounds and other metal salts, plays a significant role in the nucleation and growth of the products, resulting in $\text{Cu}_{31}\text{S}_{16}$ and CuO nanocrystals with different morphologies and size. With the phase transition from CuO to $\text{Cu}_{31}\text{S}_{16}$, the DDT and hydroxyl ions are essential influencing factors. Moreover, the two-phase approach was also extended to prepare Ag_2S and Ni_9S_8 nanocrystals, which are rarely reported in previous works. This study may open up a new strategy for synthesis of metal sulfide nanocrystals with controlled crystal phases and morphologies.

2. Experimental

2.1 Materials

Cupric nitrate trihydrate ($\text{Cu}(\text{NO}_3)_2 \cdot 3\text{H}_2\text{O}$), cupric chloride dehydrate ($\text{CuCl}_2 \cdot 2\text{H}_2\text{O}$), sodium chloride (NaCl), sodium acetate anhydrous (NaAc), and ammonium hydroxide ($\text{NH}_3 \cdot \text{H}_2\text{O}$, 30%) were purchased from Sinopharm Chemical Reagent Co., Ltd. Cupric acetate anhydrous (CuAc_2 , 99%) was purchased from Alfa Aesar. Silver nitrate (AgNO_3 , 99%), nickel nitrate hexahydrate ($\text{Ni}(\text{NO}_3)_2 \cdot 6\text{H}_2\text{O}$), and *n*-dodecanethiol (DDT, 98%) were purchased from Aladdin Reagent Company. All the chemicals were used as purchased without any further purification.

2.2 Two-phase method to synthesize different nanocrystals

In a typical synthesis of Cu_{2-x}S nanocrystals using cuprammouium compounds as copper sources, the cuprammouium compound ($\text{Cu}(\text{NH}_3)_4^{2+}$) solution was synthesized by dropping the $\text{NH}_3 \cdot \text{H}_2\text{O}$ (30%) into 20 mL of $\text{Cu}(\text{NO}_3)_2 \cdot 3\text{H}_2\text{O}$ ($0.05 \text{ mol} \cdot \text{L}^{-1}$) aqueous solution. During the process, the solution changed from clear blue to turbid and then became clear again. After keeping the above mixture stirring for 15 min, the solution was transferred to a 50 mL of Teflon-lined autoclave, and 5 mL DDT was then added into the solution, thus a two-phase reaction system was formed. Finally, the Teflon-lined autoclave was sealed and maintained at 200°C for 20 h. After the reaction was finished, the autoclave was cooled naturally to room temperature. The products were collected by adding ethanol and centrifugation at 6000 rpm for 10 min. The precipitation was re-dispersed in chloroform and collected by adding ethanol and centrifugation. The purification was repeated three times. Finally the products were dispersed in chloroform or dried in vacuum for further characterization. To study the effects of the amount of DDT and reaction rate on the formation of $\text{Cu}_{31}\text{S}_{16}$ nanocrystals, different samples were synthesized by using different DDT volumes of 1 mL, 1.5 mL and 2 mL or by introducing 5 mL toluene into the organic phase while other conditions were kept the same. Moreover, different products were also synthesized by using $\text{Cu}(\text{NO}_3)_2$, CuAc_2 and CuCl_2 as copper sources or by introducing other metal salts with different anions, such as NaCl and NaAc , in while other reaction conditions remained unchanged.

For the synthesis of Ag_2S nanocrystals, silver ammonia solution and AgNO_3 were used as the Ag sources, and 2 mL DDT or 2 mL DDT in 5 mL toluene was used as organic phase. The other reaction conditions were kept the same as the synthesis of Cu_{2-x}S nanocrystals.

For the synthesis of Ni_9S_8 nanocrystals, $\text{Ni}(\text{NO}_3)_2$ aqueous solution was used for the Ni sources, and 2 mL DDT was used to form the two-phase system. The other conditions were kept the same as that of synthesis of Cu_{2-x}S nanocrystals.

2.3 Characterizations

Powder X-ray diffraction (XRD) patterns were taken on a Bruker D8 Discover X-ray diffractometer with a $\text{Cu K}\alpha$ radiation source ($\lambda=1.54056 \text{ \AA}$). The transmission electron microscopy (TEM) was taken on a Hitachi-7650 TEM operating at an accelerating voltage of 100 kV. The high-resolution TEM (HRTEM) images were taken on a JEM-2010 at an accelerating voltage of 200 kV. The X-Ray photoelectron spectroscopy (XPS) measurement was collected on Thermo escalab 250Xi XPS spectrometer using non-monochromatic $\text{Al K}\alpha$ (1486.6 eV). The Fourier transform infrared (FT-IR) spectra were collect by a Nicolet-6700 spectrometer. The UV-Vis-NIR absorption spectra of the samples in chloroform were recorded using a Varian 5000 spectrophotometer. All of the measurements were performed at room temperature.

3. Result and discussion

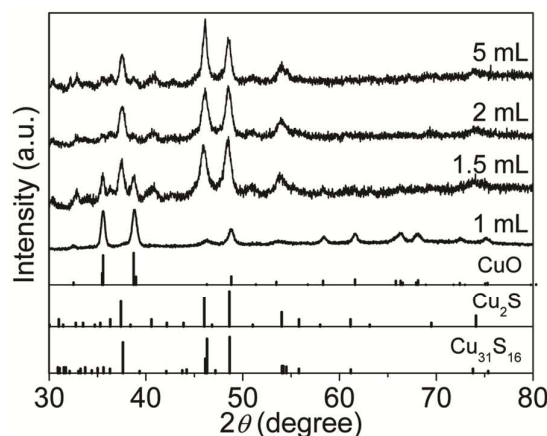


Fig. 1 XRD patterns of the products synthesized using $\text{Cu}(\text{NH}_3)_4^{2+}$ as Cu sources in the presence of different volumes of DDT, and the bottom lines represent the standard diffraction lines of monoclinic CuO (JCPDS No. 89-5895), orthorhombic Cu_2S (JCPDS No. 09-0328) and monoclinic $\text{Cu}_{31}\text{S}_{16}$ (JCPDS No. 23-0959).

To study the effects of the dosage of DDT on the nucleation and growth process of the products, a series of experiments have been carried out by varying the dosage of DDT while $\text{Cu}(\text{NH}_3)_4^{2+}$ is used as Cu sources. Fig. 1 depicts the XRD patterns of the products synthesized in the presence of different dosage of DDT. When the volume of DDT is 1 mL, all the diffraction peaks of the as-obtained products can be indexed as pure monoclinic CuO (JCPDS No. 89-5895). As the volume of DDT is increased to 1.5 mL, two typical diffraction peaks of CuO at $2\theta=35.5^\circ$ and 38.7° become weak, and a new diffraction peak between them appears. Moreover, the diffraction peaks at $2\theta=45.2^\circ$ and 47.6° become dominant in the XRD patterns, and a weak but non-ignorable diffraction peak at $2\theta=40.8^\circ$ is also observed. Further increasing the dosage of DDT to 2 and 5 mL, the characterized diffraction peaks almost disappear, and all the diffraction peaks can be assigned to djurleite ($\text{Cu}_{31}\text{S}_{16}$) (JCPDS No. 23-0959) or α -chalcocite (Cu_2S) phase (JCPDS No. 09-0328). As a matter of fact, the diffraction peaks of the djurleite ($\text{Cu}_{31}\text{S}_{16}$) and α -chalcocite (Cu_2S) are very

similar, in which some diffraction peaks are overlapped.⁴⁰ Therefore, it is difficult to distinguish α -chalcocite from djurleite. However, the intensity of the diffraction peak $2\theta=40.8^\circ$ in α -chalcocite is stronger than that in djurleite phase, thus the appearance of the diffraction peak $2\theta=40.8^\circ$ demonstrates that Cu_2S phase is present in the products synthesized by using the dosage of 2 and 5 mL of DDT. On the other hand, the LSPR absorption result shown in Fig. 4 suggests the presence of $\text{Cu}_{31}\text{S}_{16}$, which will be discussed in detail in the following part. The XRD results indicate that the crystal phase of the as-obtained products synthesized by using $\text{Cu}(\text{NH}_3)_4^{2+}$ as Cu sources transforms from copper oxide to Cu_{2-x}S nanocrystals with the increasing of the dosage of DDT.

To explore the growth process of the products synthesized using $\text{Cu}(\text{NH}_3)_4^{2+}$ as Cu sources through this two-phase approach, FT-IR spectra have been measured. Herein, we take the products synthesized in the presence of 5 mL of DDT as an example, and the FT-IR spectra of the intermediate sample (10 h) and the final product (20 h) are given in Fig. S1†. Two bands at 2924 and 2847 cm^{-1} are observed in the intermediate sample, which can be ascribed to the asymmetric methyl stretching vibration and the asymmetric and symmetric methylene stretching modes.⁴¹ Both the two bands become weak in the final products after reaction for 20 h. In addition, the band at 722 cm^{-1} is observed in the intermediate sample belonging to S-C bond disappears in the final product, which indicates the break of S-C bond and the formation of Cu_{2-x}S nanocrystals.⁴¹

The morphology of the as-obtained products has been examined by employing TEM techniques. Fig. 2 shows the TEM images of the products synthesized by using $\text{Cu}(\text{NH}_3)_4^{2+}$ as Cu sources in the presence of different dosage of DDT. As shown in Fig. 2a, the nanocrystals synthesized in the presence of 1 mL DDT exhibit a spherical shape with a relatively uniform size distribution, and the mean size is measured to be about 4.0 nm based on 100 particles (Fig. S2a†). When the volume of DDT is increased from 1 mL to 1.5 mL, the products are still kept a spherical shape but the size distribution becomes inhomogeneous. In combination with the XRD results, the uneven size distribution can be attributed to the coexistence of the CuO and Cu_{2-x}S nanocrystals. To distinguish Cu_{2-x}S nanocrystals from CuO nanocrystals, the corresponding HRTEM images have been measured, which are given in Fig. 2e and f, respectively. The HRTEM image of a single relatively large nanoparticle shown in Fig. 2e indicates its good crystallinity, and the lattice spacing of 0.196 nm is in accordance with the (080) planes of monoclinic $\text{Cu}_{31}\text{S}_{16}$ or the (600) planes of orthorhombic Cu_2S . On the other hand, the lattice spacing of 0.19 nm shown in Fig. 2f can be assigned to the ($\bar{2}02$) planes of monoclinic CuO, which suggests that the small-sized nanocrystals should be indexed as CuO nanocrystals. Further increasing the dosage of DDT to 2 and 5 mL, monodispersed spherical nanocrystals are observed in the TEM images shown in Fig. 2c and d, and the mean size is measured to be 13.9 ± 1.7 to 22.1 ± 2.6 nm by counting 100 particles (Fig. S2c†). The aforementioned results indicate that the dosage of DDT plays a significant role in the manipulation of the composition, crystal phase and morphology of the products synthesized by such a two-phase approach.

XPS technique has been employed to study the composition and valence state of the products synthesized by using different dosage of DDT. Fig. 3 shows the high-resolution XPS spectra of Cu 2p, S 2p and O 1s of the typical three samples synthesized by using 1 mL, 1.5 mL and 5 mL of DDT. As shown in Fig. 3a, there are two symmetric and narrow binding energy peaks at 952.4 and 932.7 eV, corresponding to the characteristic Cu 2p_{1/2} and Cu 2p_{3/2}. It should be noted that a weak but non-ignorable satellite peak is observed between the Cu 2p_{1/2} and Cu 2p_{3/2} peaks in the products synthesized by using 1 mL and 1.5 mL of DDT (Fig. S3†), which indicates the presence of Cu(II) in both the two products.^{42, 43} In contrast, such a satellite peak is absent in the product synthesized by using 5 mL of DDT, which rules out the presence of Cu(II) and confirms the formation of $\text{Cu}_{31}\text{S}_{16}$, matching well with our previous results.^{18, 28} The binding energy peaks of S 2p shown in Fig. 3b were fitted into two peaks (S 2p_{1/2} and S 2p_{3/2}) by using a spin-orbit separation of 1.1 eV, which may arise from the S ions coordinated to metal ions and the chemically bound thiolate sulfur, respectively.^{28, 29} Considering the fact that the CuO was formed in the samples synthesized in the presence of 1 mL and 1.5 mL of DDT, the XPS result of O 1s is an important evidence for confirming the formation of CuO phase. The O 1s peak of the samples synthesized by using 1 mL and 1.5 mL of DDT is fitted into two peaks at 531.8 and 531 eV, which can be assigned to the adsorbed oxygen and lattice oxygen in CuO, respectively.⁴⁴ Moreover, the O 1s peak of the sample synthesized in the presence of 5 mL of DDT is fitted into two peaks at 533 and 531.7 eV, which may originate from the adsorbed H₂O and surface -OH groups.⁴⁴ Additionally, the atomic ratio of Cu to S in the sample was calculated to be 1.98:1 based on the XPS results. To further confirm the Cu:S atomic ratio, the corresponding EDS data is given in Fig. S4†, which indicates that the Cu:S atomic ratio is 1.99:1, which is in good agreement with the XPS result. This result confirms the coexistence of djurleite and α -chalcocite in the product.

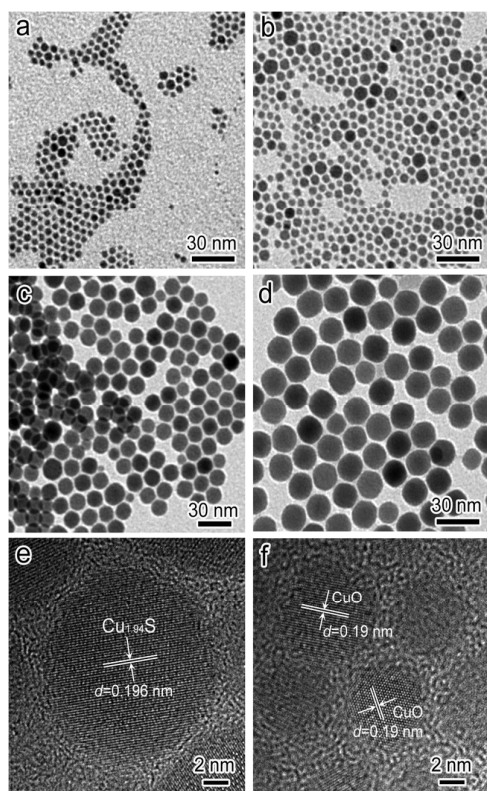


Fig. 2 TEM images of the products synthesized using $\text{Cu}(\text{NH}_3)_4^{2+}$ as Cu sources in the presence of different volumes of DDT: (a) 1 mL; (b) 1.5 mL; (c) 2 mL; (d) 5 mL, together with the HRTEM images of (e) the larger particle and (f) the smaller particle shown in Fig. 2b.

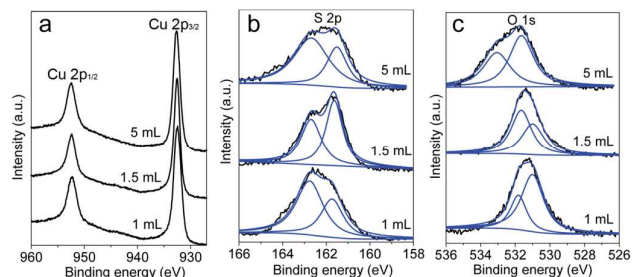


Fig. 3 XPS spectra of the products synthesized using $\text{Cu}(\text{NH}_3)_4^{2+}$ as Cu sources in the presence of different volume of DDT: (a) Cu 2p; (b) S 2p; (c) O 1s.

Very recently, localized surface plasmon resonance (LSPR) in the NIR region has been observed in Cu_{2-x}S nanocrystals in a number of literatures due to excess holes in the valence band caused by Cu deficiencies.^{19, 45–48} Therefore, LSPR absorption spectroscopy is a convincing tool to distinguish the CuO, Cu_3S_{16} and Cu_2S nanocrystals. As shown in Fig. 4a, an obvious absorption peak of 337 nm is detected in the product synthesized in the presence of 1 mL of DDT, which exhibits an obvious blue-shift as compared to the bulk CuO due to the quantum confinement effect.⁴⁹ Comparably, there are no characteristic absorption peaks observed in the region of 300–500 nm for other samples (Fig. 5†). As shown in Fig. 4b, the CuO nanocrystals have no evident absorption peak beyond 500 nm, but a broad and apparent absorption peak in the NIR region is observed in the samples synthesized by using 1.5 mL and 2 mL DDT which can be attributed to the LSPR absorption of Cu_3S_{16} phase in the samples. In combination with the XRD results, the products synthesized in the presence of 2 and 5 mL of DDT are the mixture of Cu_3S_{16} and Cu_2S phases. Obviously, the LSPR absorption peak blue-shifts from 1640 nm to 1387 nm with the volume of DDT increasing from 1.5 mL to 2 mL, and the LSPR absorption intensity is enhanced greatly, which may arise from the increasing particle size and the complete phase transition from CuO to Cu_3S_{16} . The optical absorption results confirm once again that the composition and crystal phase of the product transforms from CuO to copper (I) sulfide nanocrystals with the amount of DDT increasing when the $\text{Cu}(\text{NH}_3)_4^{2+}$ is used as Cu sources.

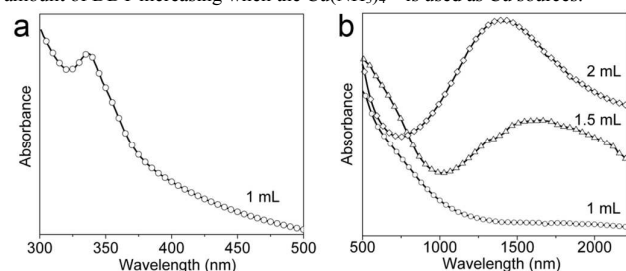


Fig. 4 (a) UV-Vis absorption spectrum of CuO nanocrystals synthesized using $\text{Cu}(\text{NH}_3)_4^{2+}$ in the presence of 1 mL DDT; (b) LSPR absorption spectra on the of the products using $\text{Cu}(\text{NH}_3)_4^{2+}$ as Cu sources in the presence of different volumes of DDT.

Based on the experimental results mentioned above, a plausible reaction mechanism is proposed as follows: in the two-phase reaction, the DDT is the upper phase and the aqueous solution of $\text{Cu}(\text{NH}_3)_4^{2+}$ ions is the lower phase, thus the water/oil interface formed. In the aqueous phase, the $\text{Cu}(\text{NH}_3)_4^{2+}$ can be dissociated into Cu^{2+} in the alkaline condition, and then Cu^{2+} ions can migrate to the water/oil interface. In general, the DDT serves as the capping

ligands, sulfur sources and reducing agent in the synthesis of metal sulfide nanocrystals, and it's no exception in our case.^{18, 28} In the oil phase, the -SH part of the DDT molecules is close to the aqueous phase because the aliphatic chain is hydrophobic, and the DDT can self-assemble around the metal ions to form monolayer-capped metal clusters through the S atoms, which can serve as the nuclei to grow up at the water/oil interface. Previous work reported by Ji's group suggested that the hydroxyl ions played an important role in the formation of oxides.⁵⁰ Herein, the presence of hydroxyl ions is also important for the nucleation of the products. As a matter of fact, the DDT and hydroxyl ions can coordinate with Cu^{2+} to form the nanocrystal nuclei, which is a competitive process and has a close association with the concentration of DDT and hydroxyl ions. When the dosage of DDT is low, such as 1 mL, the DDT mainly acts as the surface capping ligands. In the aqueous phase, the as-formed metal cluster and hydroxyl ions migrate to the water/oil interface, both of them can combine together to form a DDT-capped (Cu+O:) cluster serving as the nuclei and grow up to CuO nanocrystals. Due to the intrinsic hydrophobic property of the capping ligands, the nanocrystals could be pulled into the oil phase and thus they can disperse in the non-polar solvent.³⁸ The formation of CuO nanocrystals has been confirmed by the XRD, XPS and the optical absorption results. In contrast, when the dosage of DDT is high, plenty of DDT molecules can spread over the interface, which can offer enough hydron to promote the dissociation of $\text{Cu}(\text{NH}_3)_4^{2+}$ into more Cu^{2+} ions. Therefore, the DDT has enough opportunity to coordinate with the Cu^{2+} to form Cu-DDT compound and then decompose into Cu_3S_{16} , in which the DDT acts as the reducer and sulfur sources. This can be confirmed by the XRD, XPS and LSPR absorption results.

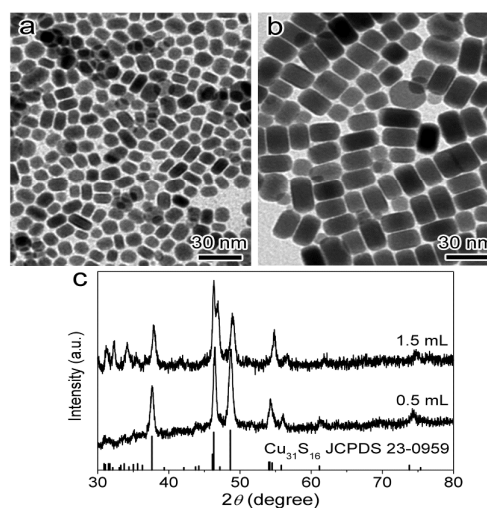


Fig. 5 TEM images of the products synthesized using $\text{Cu}(\text{NO}_3)_2$ as Cu sources in the presence of different volume of DDT: (a) 0.5 mL; (b) 1.5 mL and (c) the corresponding XRD patterns together with the standard diffraction lines of monoclinic Cu_3S_{16} (JCPDS No. 23-0959).

Now that the hydroxyl ions take part in the formation of CuO nanocrystals when the dosage of DDT is low, can the CuO nanocrystals be formed in the absence of hydroxyl ions? To verify the effect of hydroxyl ions on the formation of CuO nanocrystals, $\text{Cu}(\text{NO}_3)_2$ was used as the Cu sources directly in the control experiments while other reaction conditions were kept the same. Fig. 5 shows the TEM images and XRD patterns of the

products synthesized in the presence of 0.5 mL and 1.5 mL of DDT. Interestingly, the morphology and crystal phase of the products synthesized using $\text{Cu}(\text{NO}_3)_2$ as Cu sources are very different from those of the samples synthesized using $\text{Cu}(\text{NH}_3)_4^{2+}$. As shown in Fig. 5a and b, the as-obtained products exhibit a rod-like shape at first glance, but they are composed of nanodisks perpendicular to the substrate by careful observation, which can be confirmed by some particles with their face parallel to the substrates. The mean length and thickness of the nanodisks increase from 11.8 ± 2.2 to 24.1 ± 3.2 nm, 7.1 ± 1.0 to 14.1 ± 1.0 nm, respectively (Fig. S6†). The XRD patterns shown in Fig. 5c indicate that the products have a monoclinic Cu_3S_{16} phase, and no obvious diffraction peaks assigned to CuO are observed. As compared to the products synthesized in the presence of $\text{Cu}(\text{NH}_3)_4^{2+}$, the formation of Cu_3S_{16} nanodisks is preferential in the samples synthesized in the presence of Cu^{2+} , even if the dosage of DDT is as low as 0.5 mL. Herein, the Cu^{2+} ions can migrate to the water/oil interface much faster than that in the presence of $\text{Cu}(\text{NH}_3)_4^{2+}$, and the DDT molecules can self-assemble around the Cu^{2+} to form DDT-capped metal clusters. Due to the absence of hydroxyl ions in the interface, the metal clusters have no opportunity to react with the hydroxyl ions to form (Cu+O) cluster, thus the CuO phase can't be formed in the absence of hydroxyl ions. Therefore, the hydroxyl ions play an important role in the formation of oxides in the two-phase system.

Fig. 6 displays the LSPR absorption spectra of the Cu_3S_{16} nanodisks synthesized by using $\text{Cu}(\text{NO}_3)_2$ as Cu sources. The LSPR spectrum of the samples synthesized in the presence of 0.5 mL of DDT exhibits a peak wavelength near 1600 nm, which can be assigned to the out-of-plane LSPR mode according to previous reports.⁴⁵ When the volume of DDT is increased to 1.5 mL, the LSPR band blue-shifts to about 1500 nm, and the broadening of the LSPR band may arise from the morphology change. The corresponding LSPR absorption spectra versus energy scale are given in the inset, which have been fitted to a Gaussian function.

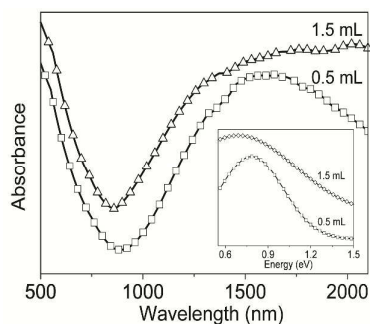


Fig. 6 UV-Vis absorption spectrum of the products synthesized using $\text{Cu}(\text{NO}_3)_2$ as Cu sources in the presence of different volume of DDT: 0.5 mL; 1.5 mL and the corresponding energy scale is shown in inset.

As aforementioned that the nucleation stage was a competitive process, in which the DDT and hydroxyl ions could take part in the formation of nuclei, respectively. To further demonstrate this plausible deduction, some contrast experiments have been designed and conducted by introducing 5 mL of toluene into the oil phase, in which the volume of DDT is kept at 1 mL and 2 mL, respectively. Fig. 7 displays the TEM images and XRD patterns of the products synthesized by using $\text{Cu}(\text{NH}_3)_4^{2+}$ as Cu sources. As shown in Fig. 7a, the samples synthesized in the presence of 1 mL of DDT are spherical in shape with a uniform size distribution. The corresponding

XRD patterns shown in Fig. 7c indicate that all the diffraction peaks match well with the monoclinic CuO phase. Further increasing the volume of DDT to 2 mL gives rise to an uneven size distribution, in which some small nanocrystals coexist in the relatively large nanocrystals (Fig. 7b). Accordingly, the monoclinic CuO phase dominates over the XRD patterns of the sample (Fig. 7c), but some diffraction peaks of Cu_3S_{16} phase are still detected, which indicates that the as-obtained sample is a mixture of CuO and Cu_3S_{16} nanocrystals. In contrast, the monoclinic Cu_3S_{16} is the main phase in the corresponding samples synthesized without toluene (Fig. 1) while the monodispersed nanocrystals are spherical. All the information suggests that the toluene is of vital importance for the nucleation and growth of the metal sulfide nanocrystals via a two-phase approach.

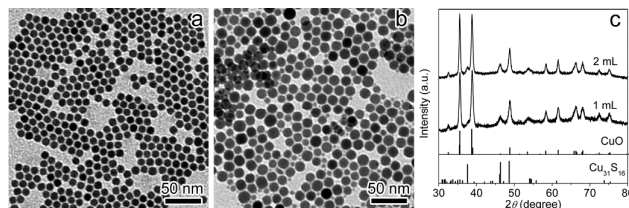


Fig. 7 TEM images of the products synthesized using $\text{Cu}(\text{NH}_3)_4^{2+}$ as Cu sources in the presence of 5 mL toluene for the different volume of DDT: (a) 1 mL; (b) 2 mL and (c) the corresponding XRD patterns together with the standard diffraction lines of monoclinic CuO (JCPDS No. 89-5895) and monoclinic Cu_3S_{16} (JCPDS No. 23-0959).

To gain further insight into the function of the toluene in the synthesis of Cu_3S_{16} nanocrystals, some control experiments have also been performed in which the $\text{Cu}(\text{NO}_3)_2$ acts as the Cu sources in the presence of 5 mL of toluene. The corresponding TEM images and XRD patterns of the samples are depicted in Fig. 8, in which the volume of DDT is 1 and 2 mL. As shown in Fig. 8a and b, different-sized particles are present in the sample synthesized in the presence of 1 mL of DDT, and monodispersed nanodisks are obtained in the sample synthesized by using 2 mL of DDT. The XRD patterns of both the samples shown in Fig. 8c agree well with the observation from TEM images. The sample prepared in the presence of 1 mL of DDT is a mixture of monoclinic CuO (JCPDS No. 89-5895) and cubic Cu_2O (JCPDS No.78-2076). But the sample synthesized in the presence of 2 mL is indexed as pure monoclinic Cu_3S_{16} , and no other impurities, such as CuO and Cu_2O are observed. HRTEM images shown in Fig. 8c and d have been employed to distinguish the different-sized particles (Fig. 8a), and the distances between the two adjacent spacing are measured to be 0.187 nm and 0.213 nm, which are ascribed to (202) plane of monoclinic CuO and (200) plane of cubic Cu_2O , which are consistent with the XRD results. By comparison with the TEM and XRD results of the samples synthesized with and without toluene in the organic phase, a big difference takes place in the morphology and crystal phase. The morphology is disk-like and the Cu_3S_{16} is the main phase in the samples synthesized without any toluene in the organic phase (Fig. 5), however, the oxides appear in the sample synthesized in the presence of toluene when the dosage of DDT is 1 mL, which implies that the incorporation of toluene into the organic phase has a significant effect on the formation of metal sulfide nanocrystals via such a two-phase approach. As a matter of fact, the boiling point of toluene (~ 110 °C) is lower than the reaction temperature (200 °C), and the volatilization of the toluene can take the DDT away from the water/oil interface, thus the opportunities of the DDT coordination with Cu^{2+} are decreased greatly. As a result, some Cu^{2+} ions at the water/oil interface can be oxidized by the oxygen in the reaction system. On the other hand,

some Cu^{2+} can also be reduced by DDT at the interface, resulting in the formation of Cu_2O nanocrystals. When the dosage of DDT reaches up to as high as 2 mL, although some DDT can be taken away from the interface through the volatilization of toluene, yet other DDT spread over the interface, resulting in the formation of $\text{Cu}_{31}\text{S}_{16}$ nanocrystals. Besides, there are significant differences in the morphology and crystal phase of the samples synthesized by using $\text{Cu}(\text{NH}_3)_4^{2+}$ and $\text{Cu}(\text{NO}_3)_2$ as Cu sources in the presence of toluene in the organic phase, which also confirms that the reactivity of Cu precursors influences the nucleation and growth greatly and the presence of hydroxyl ions is very important for the formation of CuO nanocrystals.

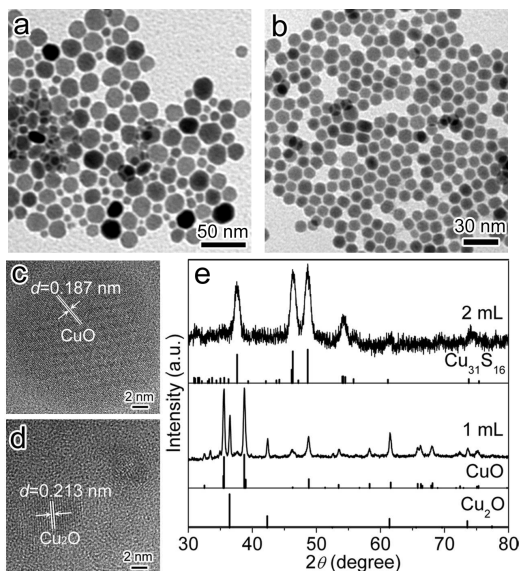


Fig. 8 TEM images of the products synthesized using $\text{Cu}(\text{NO}_3)_2$ as Cu sources in the presence of 5 mL toluene for the different volume of DDT: (a) 1 mL; (b) 2 mL and the representative HRTEM images of (c) larger particle and (d) smaller particle shown in Fig. 6a, (e) the corresponding XRD patterns together with the standard diffraction lines of monoclinic CuO (JCPDS No. 89-5895), Cu_2O (JCPDS No.78-2076) and monoclinic $\text{Cu}_{31}\text{S}_{16}$ (JCPDS No. 23-0959).

Apart from the effects of the dosage of DDT, the hydroxyl ions and the incorporation of toluene into the organic phase on the nucleation and growth of the nanocrystals, the anions in the reaction system have also affect the nucleation and growth of the products. Firstly, the products have been synthesized by using $\text{Cu}(\text{NH}_3)_4^{2+}$ and 2 mL of DDT in the presence of NaAc and NaCl. The TEM and XRD results shown in Fig. S7† indicate that the products are spherical with a narrow size distribution, and all the diffraction peaks match well with the monoclinic $\text{Cu}_{31}\text{S}_{16}$ phase, which is consistent with the results without any other added anions. These results suggest that the other added anions have a negligible effect on the crystal phase and morphology of the products. In contrast, when CuCl_2 and CuAc_2 were used to replace $\text{Cu}(\text{NO}_3)_2$ as Cu sources while other reaction conditions were kept the same, the corresponding TEM images and XRD patterns are given in Fig. S8†. Large-sized nanodisks are observed in Fig. S8a†, and the disk-like shape is affirmed by some particles with their faces perpendicular to the substrate (inset of Fig. S8a†). The XRD results show that the monoclinic $\text{Cu}_{31}\text{S}_{16}$ is the dominant phase but some non-negligible diffraction peaks assigned to CuO phase is also found. However, monodispersed $\text{Cu}_{31}\text{S}_{16}$ nanospheres are obtained in the presence of CuAc_2 , which can be testified

by the XRD and TEM results shown in Fig. S8b† and c†. Furthermore, the nanocrystals have a high tendency to self-assemble into highly-ordered superlattices (inset of Fig. S8b†). Based on the above results, the Cl^- ions have a more remarkable effect on the formation of $\text{Cu}_{31}\text{S}_{16}$ nanocrystals. As stated by Zhuang et al in the previous report that the Cl^- and Ac^- ions had different coordinating abilities and affect the reaction rate, which could result in the different size of the products. In addition, the Cl^- ions can be preferentially adsorbed on some specific facet, which brings about the anisotropic growth of the particles.³⁹

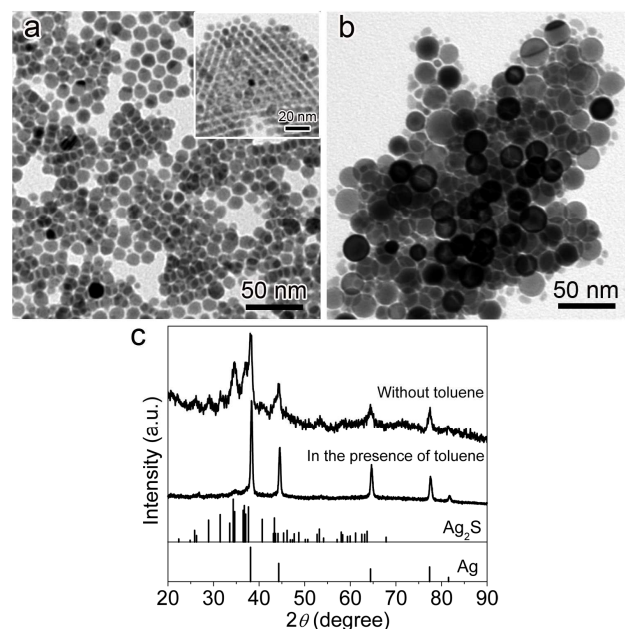


Fig. 9 TEM images of the products synthesized (a) without toluene and (b) in the presence of toluene; (c) the XRD patterns of the products synthesized with or without toluene, and the bottom lines represent the standard diffraction lines of monoclinic Ag_2S (JCPDS No. 14-0072) and metallic Ag (JCPDS No.04-0783).

It is well known that Ag and Cu belong to the same group, it is predicted that this two-phase approach may be extended to prepare Ag_2S nanocrystals. Fig. 9 gives the TEM images and XRD patterns of the products synthesized with and without toluene in the organic phase, in which 1 mmol of AgNO_3 and 2 mL of DDT were used as Ag source and S source, respectively. As shown in Fig. 9a, the products synthesized without any toluene exhibit a quasi-spherical shape with a relatively-large size distribution. Interestingly, the nanospheres can self-assemble into highly-ordered superlattices (inset of Fig. 9a). Based on our previous work, the self-assembly behavior may arise from the presence of excess DDT due to the cohesive interaction through interdigitation or interpenetration of alkyl chains of thiol molecules.²² The corresponding XRD results shown in Fig. 9c indicate that the Ag_2S is the main phase of the products synthesized without toluene, and some diffraction peaks assigned to Ag phase can also be observed, which is in good agreement with the TEM results shown in Fig.9a. In contrast, large-sized nanospheres are dominant in the TEM images of the products synthesized in the presence of toluene, and some small-sized particles appear around the large-sized nanospheres (Fig. 9b). On the other hand, the diffraction peaks assigned to metallic Ag phase are dominated over the XRD patterns shown in the Fig. 9c, in which some non-ignorable diffraction peaks of Ag_2S phase are also observed. The aforementioned results indicate that

the presence of toluene in the organic phase has a significant effect on the formation of Ag_2S and Ag nanocrystals, which is consistent with our previous work through a simple heat-up approach.²² As stated in our previous work, the Ag_2S and Ag nanocrystals can be controllable synthesized by varying the dosage of DDT, which has a vital effect on the cleavage of S-C and Ag-S.²² Similar to the case of djurite nanocrystals synthesized with and without toluene the introduction of toluene in the reaction system could decrease the amount of DDT on the water/oil interface, the cleavage of Ag-S bond is preferential. Otherwise, the nucleophilic attack of DDT takes place, which leads to the cleavage of S-C, resulting the formation of Ag_2S nanocrystals. The absorption spectra shown in Fig. S9† also confirm the Ag nanocrystals are the main phase in the presence of toluene, and the Ag and Ag_2S coexist in the products synthesized without toluene. In addition, if we used $\text{Ag}(\text{NH}_3)^+$ as Ag sources, the Ag and Ag_2S phases coexist in the as-obtained products synthesized by using 1 mmol of $\text{Ag}(\text{NH}_3)^+$ and 2 mL of DDT in the absence of toluene (Fig. S10a†). Two different-sized nanospheres are observed in the TEM images of Fig. S10b† of SI, in which some small-sized nanoparticles are self-assembled into highly-ordered superlattices.

Except for the metal sulfide nanocrystals in the same group, this two-phase approach can also be extended to the synthesis of other metal sulfides. Herein, we take the preparation of Ni_9S_8 nanocrystals as an example, in which 1 mmol of $\text{Ni}(\text{NO}_3)_2$ and 2 mL of DDT were used. Fig. 10 depicts the XRD patterns and TEM images of the products. All the diffraction peaks shown in Fig. 10a match well with single phase orthorhombic Ni_9S_8 (Godlevskite, JCPDS No. 22-1193), and no other phases such as NiO or Ni are detected in the XRD patterns. The TEM images of Ni_9S_8 nanocrystals shown in Fig. 10b indicate that the nanocrystals are quasi-flower with the size over 100 nm with some nanoparticles aggregation, and the further study is going on. The results demonstrate that this two-phase method opens up a new strategy for synthesis of metal sulfide nanocrystals.

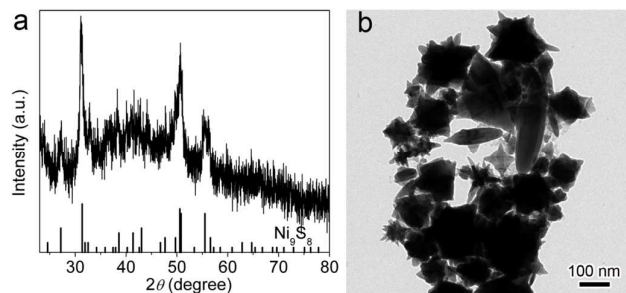


Fig. 10 (a) XRD patterns of the products synthesized by 1 mmol of $\text{Ni}(\text{NO}_3)_2$ and 2 mL of DDT with the standard diffraction peaks of orthorhombic Ni_9S_8 (JCPDS No. 22-1193) (b) corresponding TEM images.

4. Conclusions

In summary, a simple two-phase method has been developed to synthesize metal sulfide nanocrystals, in which pure DDT or DDT in toluene was selected as organic phase, and the different metal salts in water are used as aqueous phase. The nucleation and growth process can be controlled through the reactivity of metal sources and the dosage of DDT at the water/oil interfaces. The crystal phase transforms from monoclinic CuO to $\text{Cu}_{31}\text{S}_{16}$ with the increase of the dosage of DDT when the $\text{Cu}(\text{NH}_3)_4^{2+}$ is used as Cu

sources, which is confirmed by the XPS spectra and optical absorption results. The $\text{Cu}_{31}\text{S}_{16}$ nanocrystals exhibit an obvious LSPR band in the NIR region due to their excess holes in the valence band. Moreover, the volatilization of toluene can take some DDT away from the water/oil interface, which reduces the reaction of Cu sources with the DDT, and the formation of copper oxides is preferential while the oxygen and hydroxyl ions participate in the aqueous phase. Furthermore, when the copper sources are present in the aqueous phase without hydroxyl ions, the $\text{Cu}_{31}\text{S}_{16}$ nanodisks are preferentially formed, which can be affected by the anions in the copper salts. This two-phase approach has also been extended to prepare Ag_2S and Ni_9S_8 nanocrystals, which may shed light on the design and synthesis of metal sulfide nanocrystals with tailored crystal phases and morphologies.

Acknowledgements

This work is partly supported by the Fundamental Research Funds for the Central Universities (2014JBZ010), National Natural Science Foundation of China (61108063), and National Science Foundation for Distinguished Young Scholars of China (61125505). The authors (M.W) appreciate the support from the Fundamental Research Funds for the Central Universities (S15JB00380).

Notes and references

- 1 D. V. Talapin, J. S. Lee, M. V. Kovalenko and E. V. Shevchenko, *Chem. Rev.*, 2010, **110**, 389-458.
- 2 Y. Yin and A. P. Alivisatos, *Nature*, 2005, **437**, 664-670.
- 3 Y. Li, L. Jing, R. Qiao and M. Gao, *Chem. Comm.*, 2011, **47**, 9293-9311.
- 4 A. Tang, S. Qu, F. Teng, Y. Hou, Y. Wang and Z. Wang, *J. Nanosci. Nanotech.*, 2011, **11**, 9384-9394.
- 5 A. L. Rogach, N. Gaponik, J. M. Lupton, C. Bertoni, D. E. Gallardo, S. Dunn, N. Li Pira, M. Paderi, P. Repetto, S. G. Romanov, C. O'Dwyer, C. M. Sotomayor Torres and A. Eychmuller, *Angew. Chem. Int. Ed.*, 2008, **47**, 6538-6549.
- 6 I. L. Medintz, H. T. Uyeda, E. R. Goldman and H. Mattoussi, *Nat. Mater.*, 2005, **4**, 435-446.
- 7 S. Shen, Y. Zhang, Y. Liu, L. Peng, X. Chen and Q. Wang, *Chem. Mater.*, 2012, **24**, 2407-2413.
- 8 Y. Zhang, G. Hong, Y. Zhang, G. Chen, F. Li, H. Dai and Q. Wang, *ACS Nano*, 2012, **6**, 3695-3702.
- 9 Y. Wang, A. Tang, K. Li, C. Yang, M. Wang, H. Ye, Y. Hou and F. Teng, *Langmuir*, 2012, **28**, 16436-16443.
- 10 A. Tang, L. Yi, W. Han, F. Teng, Y. Wang, Y. Hou and M. Gao, *Appl. Phys. Lett.*, 2010, **97**, 033112.
- 11 Z. Zhuang, Q. Peng and Y. Li, *Chem. Soc. Rev.*, 2011, **40**, 5492-5513.
- 12 L. Qian, J. Yang, R. Zhou, A. Tang, Y. Zheng, T. K. Tseng, D. Bera, J. Xue and P. H. Holloway, *J. Mater. Chem.*, 2011, **21**, 3814-3817.
- 13 A. Tang, F. Teng, Y. Hou, Y. Wang, F. Tan, S. Qu and Z. Wang, *Appl. Phys. Lett.*, 2010, **96**, 163112.
- 14 W. Ki Bae, J. Kwak, J. Lim, D. Lee, M. Ki Nam, K. Char, C. Lee and S. Lee, *Nanotechnology*, 2009, **20**, 075202.
- 15 H. Shen, X. Bai, A. Wang, H. Wang, L. Qian, Y. Yang, A. Titov, J. Hyvonen, Y. Zheng and L. S. Li, *Adv. Funct. Mater.*, 2014, **24**, 2367-2373.
- 16 S. Ren, L. Y. Chang, S. K. Lim, J. Zhao, M. Smith, N. Zhao, V. Bulovic, M. Bawendi and S. Gradecak, *Nano. Lett.*, 2011, **11**, 3998-4002.
- 17 Y. Wang, F. Liu, Y. Ji, M. Yang, W. Liu, W. Wang, Q. Sun, Z. Zhang, X. Zhao and X. Liu, *Dalton. Trans.*, 2015, **44**, 10431-10437.
- 18 A. Tang, S. Qu, K. Li, Y. Hou, F. Teng, J. Cao, Y. Wang and Z. Wang, *Nanotechnology*, 2010, **21**, 285602.

- 19 J. M. Luther, P. K. Jain, T. Ewers and A. P. Alivisatos, *Nat. Mater.*, 2011, **10**, 361-366.
- 20 H. Ye, A. Tang, L. Huang, Y. Wang, C. Yang, Y. Hou, H. Peng, F. Zhang and F. Teng, *Langmuir*, 2013, **29**, 8728-8735.
- 21 J. Kolny-Olesiak and H. Weller, *ACS Appl. Mater. Interfaces.*, 2013, **5**, 12221-12237.
- 22 A. Tang, Y. Wang, H. Ye, Z. Chao, C. Yang, X. Li, H. Peng, F. Zhang, Y. Hou and F. Teng, *Nanotechnology*, 2013, **24**, 355602.
- 23 M. Deng, S. Shen, X. Wang, Y. Zhang, H. Xu, T. Zhang and Q. Wang, *CrystEngComm.*, 2013, **15**, 6443-6447.
- 24 Y. Zhang, Y. Du, H. Xu and Q. Wang, *CrystEngComm*, 2010, **12**, 3658.
- 25 Y. Du, B. Xu, T. Fu, M. Cai, F. Li, Y. Zhang and Q. Wang, *J. Am. Chem. Soc.*, 2010, **132**, 1470-1471.
- 26 Z. Zhuang, Q. Peng, X. Wang and Y. Li, *Angew. Chem. Int. Ed.*, 2007, **46**, 8174-8177.
- 27 P. Li, Q. Peng and Y. Li, *Chem. Eur. J.*, 2011, **17**, 941-946.
- 28 X. Li, A. Tang, L. Guan, H. Ye, Y. Hou, G. Dong, Z. Yang and F. Teng, *RSC Adv.*, 2014, **4**, 54547-54553.
- 29 H. Ye, A. Tang, C. Yang, K. Li, Y. Hou and F. Teng, *CrystEngComm.*, 2014, **16**, 8684-8690.
- 30 G. Hong, J. T. Robinson, Y. Zhang, S. Diao, A. L. Antaris, Q. Wang and H. Dai, *Angew. Chem. Int. Ed.*, 2012, **124**, 9956-9959.
- 31 S. Shen, Y. Zhang, L. Peng, Y. Du and Q. Wang, *Angew. Chem. Int. Ed.*, 2011, **50**, 7115-7118.
- 32 Y. Zhang, Y. Liu, C. Li, X. Chen and Q. Wang, *J. Phys. Chem. C.*, 2014, **118**, 4918-4923.
- 33 Q. Wang, D. Pan, S. Jiang, X. Ji, L. An and B. Jiang, *Chem. Eur. J.*, 2005, **11**, 3843-3848.
- 34 L. Hu, M. Chen, X. Fang and L. Wu, *Chem. Soc. Rev.*, 2012, **41**, 1350-1362.
- 35 D. Pan, X. Ji, L. An and Y. Lu, *Chem. Mater.*, 2008, **20**, 3560-3566.
- 36 D. Pan, S. Jiang, L. An and B. Jiang, *Adv. Mater.*, 2004, **16**, 982-985.
- 37 D. Pan, Q. Wang, S. Jiang, X. Ji and L. An, *Adv. Mater.*, 2005, **17**, 176-179.
- 38 D. Pan, Q. Wang and L. An, *J. Mater. Chem.*, 2009, **19**, 1063-1073.
- 39 Z. Zhuang, Q. Peng, B. Zhang and Y. Li, *J. Am. Chem. Soc.*, 2008, **130**, 10482-10483.
- 40 M. Lotfipour, T. Machani, D. P. Rossi, and K. E. Plass, *Chem. Mater.*, 2011, **23**, 3032-3038.
- 41 L. Yu, Y. Lv, G. Chen, X. Zhang, Y. Zeng, H. Huang and Y. Feng, *Inorg. Chim. Acta.*, 2011, **376**, 659-663.
- 42 M. Yin, C. K. Wu, Y. Lou, C. Burda, J. T. Koberstein, Y. Zhu and S. O'Brien, *J. Am. Chem. Soc.*, 2005, **127**, 9506-9511.
- 43 P. Pallavicini, G. Dacarro, P. Grisoli, C. Mangano, M. Patrini, F. Rigoni, L. Sangaletti and A. Taglietti, *Dalton. Trans.*, 2013, **42**, 4552-4560.
- 44 D. Barreca, A. Gasparotto and E. Tondello, *Surf. Sci. Spectra.*, 2007, **14**, 41-51.
- 45 S. W. Hsu, K. On and A. R. Tao, *J. Am. Chem. Soc.*, 2011, **133**, 19072-19075.
- 46 H. Ye, A. Tang, Y. Hou, C. Yang and F. Teng, *Opt. Mater. Express.*, 2014, **4**, 220.
- 47 L. Liu, H. Zhong, Z. Bai, T. Zhang, W. Fu, L. Shi, H. Xie, L. Deng and B. Zou, *Chem. Mater.*, 2013, **25**, 4828-4834.
- 48 X. Liu, X. Wang, B. Zhou, W. C. Law, A. N. Cartwright and M. T. Swihart, *Adv. Funct. Mater.*, 2013, **23**, 1256-1264.
- 49 H. Fan, L. Yang, W. Hua, X. Wu, Z. Wu, S. Xie and B. Zou, *Nanotechnology*, 2004, **15**, 37.
- 50 N. Zhao, W. Nie, J. Mao, M. Yang, D. Wang, Y. Lin, Y. Fan, Z. Zhao, H. Wei and X. Ji, *Small*, 2010, **6**, 2558-2565.

TOC Figure

